The spatial variability of soil water content in a potato field before and after spray irrigation in arid northwestern China

Tao Li, Jian-feng Zhang, Si-yuan Xiong and Rui-xi Zhang

ABSTRACT

Assessing the spatial variability of soil water content is important for precision agriculture. To measure the spatial variability of the soil water content and to determine the optimal number of sampling sites for predicting the mean soil water content at different stages of the irrigation cycle, field experiments were carried out in a potato field in northwestern China. The soil water content was measured in 2016 and 2017 at depths of 0–20 and 20–40 cm at 116 georeferenced locations. The average coefficient of variation of the soil water content was 20.79% before irrigation and was 16.44% after irrigation at a depth of 0–20 cm. The spatial structure of the soil water content at a depth of 20–40 cm was similar throughout the irrigation cycle, but at a depth of 0–20 cm a relatively greater portion of the variation in the soil water content was spatially structured before irrigation than after irrigation. The autocorrelation of soil water contents was influenced by irrigation only in the surface soil layer. To accurately predict mean soil moisture content, 40 and 20 random sampling sites should be chosen with errors of 5% and 10%, respectively.

Key words | geostatistics, potato, sampling strategy, soil water content, spatial variation

Tao Li (corresponding author)
Jian-feng Zhang
Si-yuan Xiong
Rui-xi Zhang
State Key Laboratory of Eco-hydraulics in Northwest Arid Region of China,
Xi'an University of Technology,
Xi'an 710048,
China
E-mail: *litao@xaut.edu.cn*

INTRODUCTION

Potatoes (*Solanum tuberosum* L.) are considered to be the fourth most abundant food crop in China, after rice, maize, and wheat. A total of 5,815,140 ha of farmland, mostly located in the arid northwestern region of China, were used in 2016 to cultivate potatoes with an average yield of 17.04 t/ha (FAOSTAT 2018). The scarcity of water resources in this region requires new strategies for the use of irrigation water to improve the efficiency of water use. Precision irrigation appears to be a promising way to maintain productivity while using smaller volumes of water (Longchamps *et al.* 2015). Firstly, it is necessary to determine the spatial distribution of soil water content via measurements performed using a rational sample size in the field.

There have been many studies on the spatial variability of soil water content in the field, which is an important criterion for the precision management of agricultural water. Starr (2005) reported the spatiotemporal variability of soil water content at a commercial potato farm in the United States, and the results showed that a temporal stability model explained 47% of the observed variations in soil water content. Satchithanantham *et al.* (2014) studied the effect of shallow groundwater on the spatial distribution of soil water content within the potato root zone in Canada and found that more than 92% of the crop water demand was met by capillary rise from the shallow groundwater table in a fine sandy loam. López-Vicente *et al.* (2015)

doi: 10.2166/ws.2020.006

identified the spatial patterns of topsoil water content and their temporal stability in a Mediterranean fallow rainfed cereal field and showed that neither the spatial patterns of topsoil water content nor those of changes in its value were stable in the short term. Usowicz & Lipiec (2017) examined spatial variability of soil properties and cereal yield on sandy soil and found that the spatial dependency of soil water content was strong.

The different soil sampling strategies used for determining soil water content influence estimates of daily and cumulative evapotranspiration (Bertuzzi *et al.* 1994). Moreover, a strategy for sampling soil where the sample size is small is needed to accurately calculate the properties of soil in farmland for precision agriculture. Kerry & Oliver (2007) sampled soil at four field sites in the United Kingdom, and the results suggest that sampling should follow a structured approach for mapping soil in precision agriculture. Wang *et al.* (2015) found that the root mean square error can be used to determine the number of sampling points for measuring the properties of soil on the field scale, and the rational number of sampling sites for a field study is 40. The rational number of sampling sites for measuring the properties of soil was determined by geostatistical analysis at different sampling points (Delhomme 1978; Souza *et al.* 2014; Long *et al.* 2018). Wang *et al.* (2008) estimated the necessary sample size for measuring surface soil moisture in different sampling areas in a wheat field and found that the rational number of sampling sites selected randomly from 100 observations was greater than 48 with a relative error of 5% and a confidence level of 99%. Miller *et al.* (2016) showed that the reasonable number of sampling points were 80 and 28 to estimate the soil carbon at meso-scale and macro-scale, respectively.

Under conditions in which farmland is irrigated, irrigation is one of the most important factors that affect variations in soil water content in farmland. However, studies of the spatial variability of soil water content and sampling strategies used for predicting the mean soil moisture in a potato field under conditions of sprinkler irrigation have been insufficient. Therefore, the objects of this study were (1) to assess the spatial variability of soil water content before and after spray irrigation and (2) to develop a sampling strategy for predicting mean soil moisture at different stages under conditions of spray irrigation.

MATERIALS AND METHODS

Site description and data collection

The experiment was performed in a potato field with an area of 28.26 ha in Yulin, Shaanxi Province (38° 09′ 06.11″ N, 109° 00′ 23.73″ E, altitude 1,183 m) in 2016 and 2017. This region, which is located in a temperate semiarid climatic zone with a mean annual temperature of 6.0–8.5 °C, is characterized by the topographical features of loess hill ravines. Water is in severe shortage in this region, with an average groundwater table depth of greater than 4 m and a mean annual pan evaporation of more than 2,000 mm. The mean annual precipitation is approximately 345 mm, of which 60–75% falls from July to September. The land is desert with a covering of sandy loam with a thickness of 8 cm on the surface, and the soil is well mixed from a depth of 0–40 cm. The soil particle composition is listed in Table 1.

The potato cultivar used in both years of the experiment was Shepody, which was planted from May to September at spacings of 80 cm between rows oriented south–north and 20 cm between plants. More than 90% of the fine roots of the potato plants (diameter of <2 mm) were mainly distributed in the soil layer at a depth of 5–40 cm. A center pivot irrigation system with a large sprinkler was employed. The irrigation amount was 11 mm for each irrigation event, and the total irrigation amount was 429 mm and 473 mm during the entire growing period in 2016 and 2017, respectively. The detailed irrigation schedules are shown in Table 2.

The experimental site was a circular area with a radius of 300 m with its center at the sprinkler base. A total of 96 regularly spaced sampling points with a spacing of 25 m were located along four diameters of the site, with the exception of the center of the circle; in addition, 20 sampling points were located at random positions in the experimental

Table 1 | Soil particle composition for experimental field

	0–20 cm			20–40 cm		
Year	**Clay (%)**	**Silt (%)**	**Sand (%)**	**Clay (%)**	**Silt (%)**	**Sand (%)**
2016	3.57	14.21	82.21	3.11	13.91	82.98
2017	2.70	10.38	86.92	3.18	10.74	86.08

Table 2 | Irrigation schedule and amounts during the different growing stages in 2016 and 2017

		2016		2017	
Growth stage	**Irrigation quota (mm)**	**Irrigation events**	**Irrigation amount (mm)**	**Irrigation events**	**Irrigation amount (mm)**
Germination	11	2	22	3	33
Seedling	11	6	66	6	66
Tuber formation	11	10	110	10	110
Tuber development	11	13	143	14	154
Tuber ripe	11	8	88	10	110
Whole	11	39	429	43	473

area. As a result, there was a total of 116 sampling points, as shown in Figure 1. The volumetric soil water content was measured at each sampling location at depths of 0–20 and 20–40 cm during the growing season using a time domain reflectometer sensor (Xi'an Bi Shui RV1, China), and the measured values of the volumetric soil water content were calibrated by a gravimetric method during the experimental period of each year.

Data analysis

In accordance with the respective measurement times during an irrigation event, the soil water contents were divided into two stages, namely, 1 day before irrigation (BI) and 1 day after irrigation (AI). The coefficient of variation (CV) was used to describe the overall variation in soil water content, as well as soil properties within the experimental field. For CV $\leq$10%, heterogeneity was considered to be weak, 10% < CV < 100% was considered as moderate heterogeneity, and CV $\geq$100% was considered as strong heterogeneity (Warrick & Nielsen 1980).

The spatial distribution of the soil water content at these different stages was described by fitting the sample semivariogram with three commonly used empirical models, namely, spherical, exponential, and Gaussian models. The sample semivariogram was calculated by Equation (1):

$$\gamma(h) = \frac{1}{2N(h)} \sum_{i=1}^{N(h)} [Z(x_i) - Z(x_i + h)]^2 \quad (1)$$

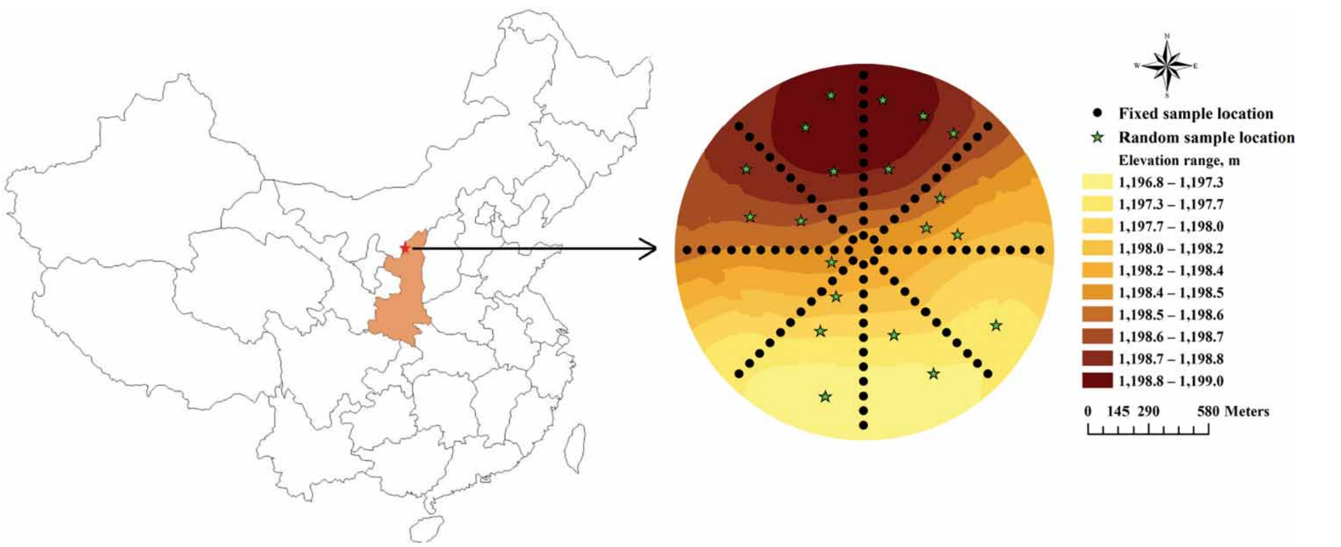

Figure 1 | Location of the experimental site in China, together with the layout of the sampling locations and an elevation map of the field.

where $\gamma(h)$ is the semivariogram for variable Z, which represents the soil water content and selected properties of soil in this study; x_i and $x_i + h$ are sampling locations separated by a distance h; $Z(x_i)$ and $Z(x_i + h)$ are the measured values of Z at the corresponding locations; and $N(h)$ is the total number of sample pairs for distance h. Details of the calculation of the semivariogram and descriptions of the models can be found in a number of studies (Burgess & Webster 1980; Cambardella *et al.* 1994; Utset *et al.* 1998; Fu *et al.* 2010).

The performance of the models was evaluated in terms of the highest coefficient of determination (R^2). In most cases, the spherical model exhibited the best performance. The average performance of the spherical model was very similar to the best performance displayed by either of the other two models. Therefore, the spherical model was used for all datasets in this study to facilitate the interpretation of the results. Calculations of semivariograms and the corresponding model fittings were conducted using Spatial Analyst for ArcGIS 10.3 software (ArcGIS 10.3, Esri, USA).

Correlogram analysis was employed to examine the autocorrelation of soil water contents between sampling points. Correlograms were calculated using GS + 9.0 software (GS + 9.0, Gamma Design Software, USA) (Robertson 2008) with the following equations:

$$\rho(h) = C(h)/(\sigma_{-h}\sigma_{+h}) \tag{2}$$

$$C(h) = [1/N(h)]\sum Z_i Z_{i+h} - m_{-h}m_{+h} \tag{3}$$

where $\rho(h)$ is the correlation for interval distance class h; σ_{+h} is the standard deviation of all head values (Z_l) for lag h_l; σ_{-h} is the standard deviation of all tail values (Z_{l+h}) for lag h_l; $C(h)$ is the covariance for interval distance class h; $N(h)$ is the total number of sample couples for lag interval h; Z_i is the measured value at sampling point i; Z_{i+h} is the measured value at sampling point $i + h$; m_{-h} is the mean of all head values for lag h; and m_{+h} is the mean of all tail values for lag h.

The random sampling strategy was used in this study: 100 random realizations of 5, 10, 20, 40, 60, 80 and 100 points with no replacement were generated from all 116 sampling points, and every point has an equal probability of being chosen. The mean soil water content can be calculated by averaging the observed soil water content at the corresponding random points on each day. The probability of accurately predicting mean soil moisture content from the random samples was calculated. The mean soil water content calculated from 116 sampling points was taken as a real value. The performances of this random sampling strategy for predicting the mean soil water content were based on the mean absolute error (MAE) and root mean square error (RMSE):

$$\mathrm{MAE} = \frac{1}{n}\sum_{i=1}^{n}|\theta_i - \widehat{\theta}_i| \tag{4}$$

$$\mathrm{RMSE} = \sqrt{\frac{1}{n}\sum_{i=1}^{n}(\theta_i - \widehat{\theta}_i)^2} \tag{5}$$

where $n = 100$; θ_i is the calculated mean soil water content from random realization, and $\widehat{\theta}_i$ is the real value of mean soil water content.

RESULTS AND DISCUSSION

Descriptive statistics of soil water content

The descriptive statistics of the volumetric soil water content on different dates in different periods of the irrigation cycle at soil depths of 0–20 and 20–40 cm in 2016 and 2017 are shown in Table 3. The lowest mean soil water content was 4.55% at a depth of 0–20 cm at the BI stage, and the highest mean soil water content was 20.86% at a depth of 20–40 cm at the AI stage. The soil water content in the experimental field was relatively low with average values of 8.71% and 12.93% at the BI and AI stages, respectively, because there was a lot of sand in the soil (Table 1). The average coefficient of variation (CV) of the soil water content over the depth range of 0–40 cm was 20.79% at the BI stage and 16.44% at the AI stage. The results for the CV of the soil water content were similar to the findings of other studies (Hupet & Vanclooster 2002; Meyles *et al.* 2003; Western *et al.* 2004; Brocca *et al.* 2010). At the BI stage the average soil water

Table 3 | Descriptive statistics of volumetric soil water content on different dates in different periods of an irrigation event at soil depths of 0–20 and 20–40 cm in 2016 and 2017

Stage	Depth (cm)	Year	Date	Mean (cm^3/cm^3, %)	Min (cm^3/cm^3, %)	Max (cm^3/cm^3, %)	SD	Skewness	CV (%)
BI	0–20	2016	13-Jul	8.26	4.74	10.95	1.53	−0.03	18.52
		2016	31-Jul	9.39	6.07	14.84	1.93	0.54	20.61
		2016	15-Aug	8.14	4.64	14.1	1.68	0.38	20.71
		2017	23-Jun	9.76	6.87	12.98	1.77	0.35	18.14
		2017	23-Jul	9.10	6.18	11.87	1.42	0.12	15.59
		2017	21-Aug	7.98	5.15	11.89	2.18	0.41	27.27
		2017	11-Sep	7.32	4.55	10.83	1.75	0.54	23.92
		Average value		8.56	5.46	12.49	1.75	0.33	20.68
	20–40	2016	13-Jul	9.05	6.02	13.62	1.8	0.27	19.87
		2016	31-Jul	11.01	5.85	18.12	2.22	−0.01	20.21
		2016	15-Aug	8.88	4.96	14.28	1.99	0.35	22.34
		2017	23-Jun	9.72	6.47	12.39	1.75	0.12	18.00
		2017	23-Jul	8.48	5.15	11.79	1.78	−0.11	20.97
		2017	21-Aug	7.18	5.02	10.43	1.41	0.52	19.63
		2017	11-Sep	7.79	4.84	11.96	1.97	0.25	25.32
		Average value		8.87	5.47	13.23	1.85	0.20	20.91
	Average value			8.71	5.46	12.84	1.80	0.27	20.79
AI	0–20	2016	15-Jul	13.38	9.36	17.29	2.12	0.23	15.87
		2016	1-Aug	13.52	9.13	17.08	2.22	−0.28	16.42
		2016	17-Aug	11.77	7.64	17.66	2.17	0.54	18.45
		2017	25-Jun	12.74	7.42	16.56	2.27	−0.06	17.79
		2017	25-Jul	11.78	9.76	15.85	1.53	0.95	13.00
		2017	23-Aug	10.31	8.84	16.52	1.52	1.90	14.74
		2017	13-Sep	11.70	9.11	15.96	1.73	0.85	14.77
		Average value		12.17	8.75	16.70	1.94	0.59	15.86
	20–40	2016	15-Jul	14.03	10.49	18.22	2.36	0.08	16.85
		2016	1-Aug	15.85	11.01	20.86	2.75	0.07	17.32
		2016	17-Aug	13.00	8.54	20.35	2.68	0.23	20.62
		2017	25-Jun	13.38	9.84	18.42	2.40	0.52	17.97
		2017	25-Jul	12.24	9.02	17.83	2.28	0.87	18.66
		2017	23-Aug	14.09	10.26	18.01	1.90	−0.08	13.48
		2017	13-Sep	14.01	10.01	18.60	2.07	0.09	14.77
		Average value		13.80	9.88	18.90	2.35	0.25	17.10
	Average value			12.93	9.28	17.73	2.13	0.43	16.44

content at depths of 0–20 cm and 20–40 cm was 8.56% and 8.87%, respectively, whereas at the AI stage the average soil water content at a depth of 0–20 cm (12.17%) was lower than that at a depth of 20–40 cm (13.80%). However, the CV values of the soil water content at depths of 0–20 cm and 20–40 cm were similar at the BI and AI stages. These results seem to suggest that during the irrigation cycle the changes in soil water content with time were relatively substantial but the level of spatial heterogeneity of the soil water content was relatively stable.

Figure 2 shows the changes in the CV with the mean soil water content. Overall, the CV increased with a decrease in the mean soil water content, as shown in Figure 2(b), whereas the slope of the trend line between the CV and soil water content at the BI stage was greater than that at the AI stage (Figure 2(a)), which indicated that when the soil water content was relatively low the level of spatial heterogeneity of the soil water content tended to be greater. This result was similar to those reported by previous studies (Famiglietti *et al.* 2008; Choi & Jacobs 2011).

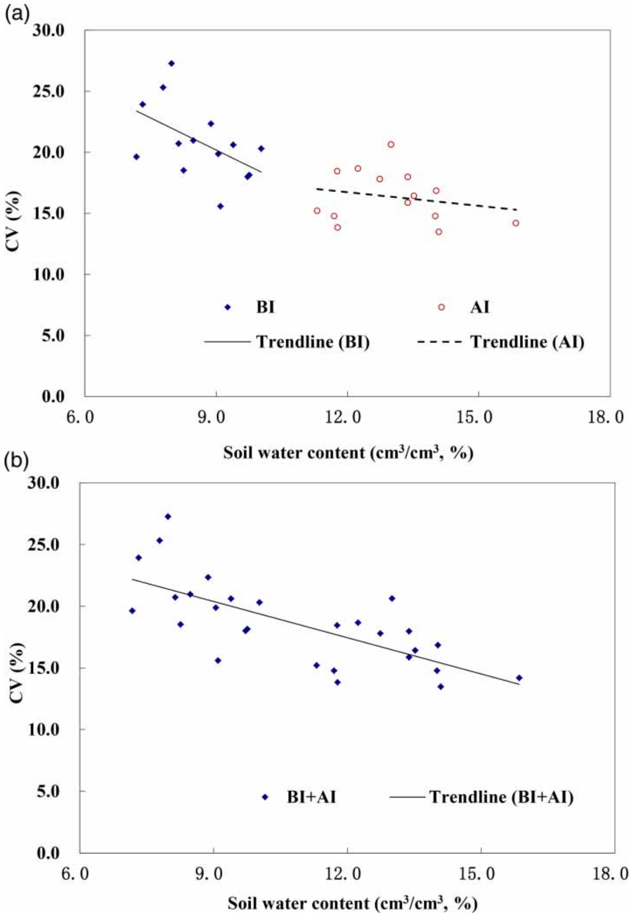

Figure 2 | Scatter plots showing trend lines for the relationship between the coefficient of variation (CV) and the mean soil water content at the different stages of the irrigation cycle: (a) separate scatter plots and trend lines for the BI and AI stages; (b) scatter plots and trend lines for all data.

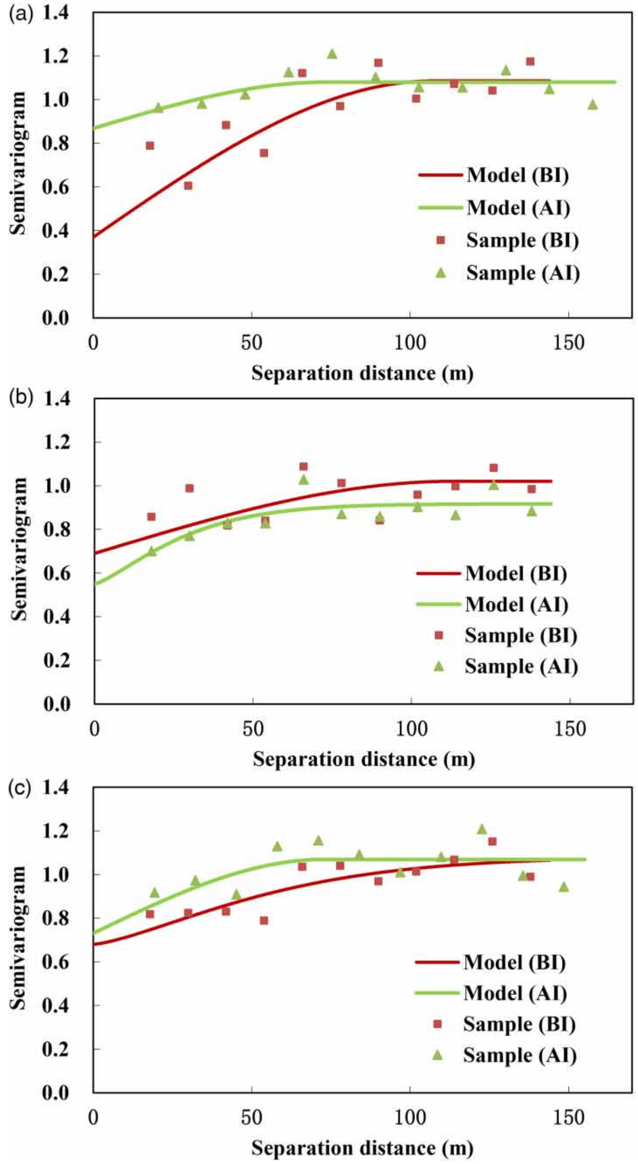

Figure 3 | Semivariograms for the standardized average soil water content at the early (BI) and late (AI) stages of the irrigation cycle at different soil depths: (a) 0–20 cm; (b) 20–40 cm; (c) 0–40 cm.

Geostatistical analysis

The sample semivariograms and the results of fitting using the spherical model, and the parameters of the fitting model used for the standardized soil water content at the early (BI) and late (AI) stages of the irrigation cycle at different soil depths are shown in Figure 3 and Table 4, respectively. The range varied from 107 to 135 m and from 71 to 74 m for the BI and AI stages, respectively, which indicated that the correlation length of the soil water content was greater for drier soil than for wetter soil. Similar results have been reported for the Da Nangou catchment in China, which is located on a loess plateau without irrigation (Wang *et al.* 2001). However, these results were inconsistent with those of Li *et al.* (2014), who found that the range was greater under wetter conditions at a soil depth of 0–20 cm under conditions of furrow irrigation in a vineyard. Under conditions of sprinkling irrigation the effect of the structure of the potato canopy on the spatial distribution of irrigation water would lead to a low spatial autocorrelation of soil water contents, which could contribute to a smaller range at the AI stage. However, under conditions of furrow irrigation the smoothing effect of furrow irrigation without the effect of the grapevine canopy would lead to a high spatial

Table 4 | The fitting nugget, sill, range, degree of spatial dependence (DSD) and coefficient of determination (R^2) for the spherical model for the semivariogram of average soil water content at BI and AI stages

Stage	Depth (cm)	Nugget	Sill	DSD (%)	Range (m)	R^2
BI	0–20	0.39	1.15	34.1	107	0.87
	20–40	0.69	1.02	67.6	113	0.94
	0–40	0.68	1.08	62.9	135	0.88
AI	0–20	0.86	1.07	80.4	74	0.86
	20–40	0.55	0.92	59.8	71	0.91
	0–40	0.73	1.06	68.9	72	0.92

DSD = nugget/sill × 100%.

autocorrelation of soil water contents, which could contribute to a larger range at the AI stage.

The degree of spatial dependence (DSD), which is defined as the ratio of the nugget value to the sill value in a semivariogram model, reflects the extent of spatial autocorrelation. If the DSD is less than 25%, a variable has strong spatial dependence; if the DSD is between 25% and 75%, it has moderate spatial dependence, whereas it has weak spatial dependence if the DSD is greater than 75% (Cambardella *et al.* 1994). At a depth of 0–20 cm the soil water content had moderate spatial dependence with a DSD of 34.1% at the BI stage but had weak spatial dependence with a DSD of 80.4% at the AI stage, which indicated that in the surface soil layer a majority of the variation (about 65%) in the soil water content was spatially structured at the BI stage, whereas only about 20% of the variation was spatially structured at the AI stage. However, at a depth of 20–40 cm the soil water content at both the BI stage and the AI stage had moderate spatial dependence with a DSD of 67.6% and 59.8%, respectively, which indicated that in the soil layer at a depth of 20–40 cm a relatively large proportion of the variation (about 37%) in the soil water content was spatially structured at the BI stage. Overall, the spatial distribution of the soil water content at a soil depth of 0–20 cm was changed by spray irrigation, which was perhaps because of the effect of the structure of the potato canopy on the uniformity of the surface soil water content during spray irrigation. However, at a soil depth of 20–40 cm the spatial distribution of the soil water content was not influenced by spray irrigation owing to the redistribution of soil water during the infiltration of water from the surface to the subsurface layer.

Spatial distribution of soil water content at BI and AI stages

Figure 4 shows the spatial distributions of the soil water content at the BI and AI stages at different soil depths. Each map was plotted on the same scale with the same contour intervals to allow easier comparisons. The soil water content at soil depths of both 0–20 cm and 20–40 cm at the AI stage was larger than that at the BI stage owing to irrigation. The soil water content at a soil depth of 0–20 cm at the BI stage and at a soil depth of 20–40 cm at the AI stage changed gradually in space in the researched region, but soil water content as a fraction of area changed suddenly at a soil depth of 0–20 cm at the AI stage and at a soil depth of 20–40 cm at the BI stage, which indicated that at a depth of 0–20 cm the spatial variability of the soil water content was higher at the AI stage than at the BI stage but at a depth of 20–40 cm it was lower at the AI stage than at the BI stage. These results agreed with the results of geostatistical analysis shown in Table 4.

Analysis of correlograms

The empirical correlograms for the mean soil water content at the BI and AI stages at different soil depths are shown in Figure 5. All the correlograms for the soil water content at different stages at different soil depths exhibited a linear decay followed by minor fluctuations about zero, which indicated that the autocorrelation of soil water contents was similar during the irrigation cycle. At a soil depth of 0–20 cm, the autocorrelation distance of the soil water content was about 70 m at the AI stage and about 140 m at the BI stage, which revealed that the spatial variability of the soil water content increased at the AI stage as a result of irrigation, which was the same result as that described above (Table 4). At a soil depth of 20–40 cm, the autocorrelation distance of the soil water content was about 60 m at both the AI stage and the BI stage, which indicated that the spatial variability of the soil water content at a soil depth of 20–40 cm remained constant owing to the redistributive effect of the surface soil on the infiltration of water. Over the soil depth range of 0–40 cm, the autocorrelation distance of the soil water content was about 70 m at both the AI stage and the BI stage.

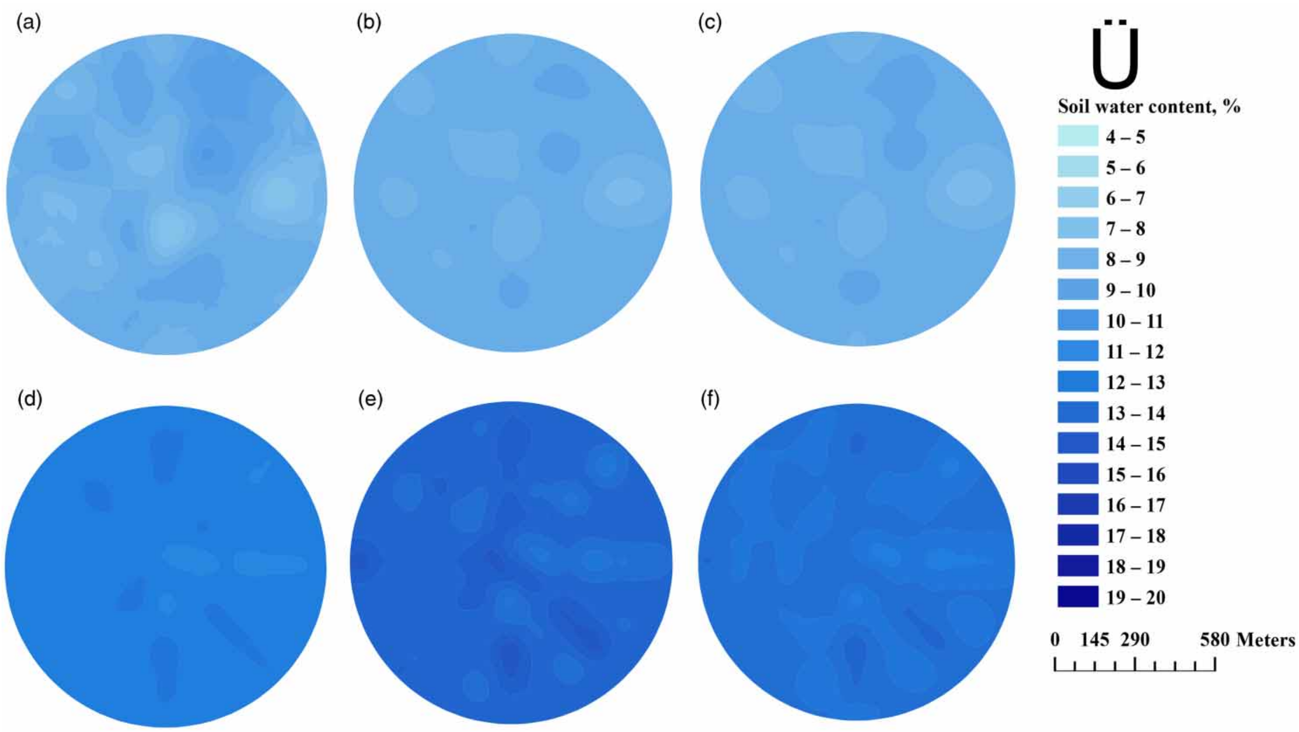

Figure 4 | Spatial distributions of average soil water content at the BI and AI stages at different soil depths: (a) BI 0–20 cm; (b) BI 20–40 cm; (c) BI 0–40 cm; (d) AI 0–20 cm; (e) AI 20–40 cm; (f) AI 0–40 cm.

Random sampling strategy for predicting mean soil moisture content

The performances of the random sampling strategy in predicting mean soil water content before and after irrigation are shown in Figure 6. When the number of points increased from 5 to 100, the MAE decreased from 0.74 to 0.06 m^3/m^3 and from 0.62 to 0.06 m^3/m^3 at AI and BI stages, respectively, indicating that the predicted mean soil water content at both AI and BI stages was more accurate with a greater number of sampling points. However, the predicted mean soil water content had a relatively smaller error at the BI stage than that at the AI stage when the same number of sampling points was selected, mainly because the spatial variability of soil water content at 0–40 cm depth was larger at AI than that at BI (Figure 3). When the number of points was less than 20, the standard deviation of soil water content at both AI and BI stages was relatively large, indicating that these sampling points were poorly representative due to the much lower number of sampling points. When the number of points was more than 40, the standard deviation of soil water content at AI stage was smaller than that at BI stage, indicating that the spatial distribution of soil water content at the BI stage was more homogeneous than that at the AI stage.

When the number of sampling points was less than 20, the RMSE of soil water content at AI stage was larger than that at BI stage, but when the number of sampling points was more than 40, the RMSE of soil water content at AI stage was smaller than that at BI stage (Figure 6(b)) due to the larger standard deviation with a greater number of sampling points at BI stage (Figure 6(a)).

Figure 7 shows the probability of the real value of mean soil water content with different random sampling number under the condition of different errors at AI and BI stages. When the number of sampling points increases from 5 to 100, the probability of the real value of mean soil water content increased at both AI and BI stages, and the maximum of probability with errors of 0% and 1% was about 11% and 85%, respectively. For the researched area at both AI and BI stages, the probability of obtaining the mean soil water content with errors of 5 and 10% with a

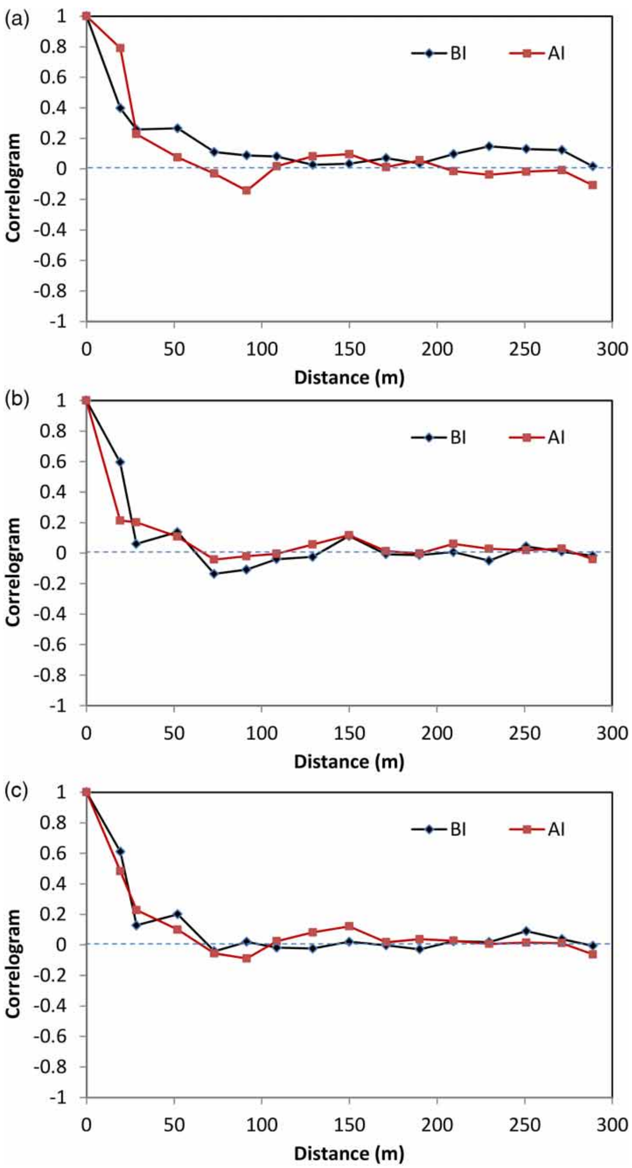

Figure 5 | Correlograms for the mean soil water content at the BI and AI stages at different soil depths: (a) 0–20 cm; (b) 20–40 cm; (c) 0–40 cm.

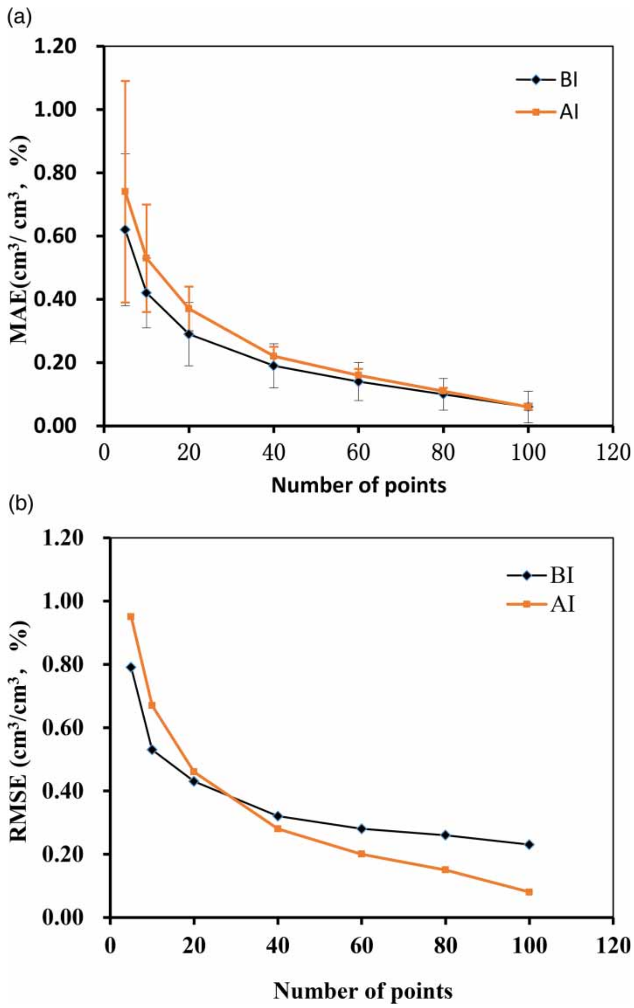

Figure 6 | The influences of sampling size on accuracy of the random sampling strategy to predict mean soil water content at AI and BI. Vertical bars correspond to standard deviation. (a) MAE; (b) RMSE.

random sampling number of more than 40 and 20, respectively, was about 100%, so this sampling strategy might result in an error of less than 1.6 cm^3/cm^3 where the range of mean soil water content is from 7.32 to 15.85 cm^3/cm^3 (Table 3), and this magnitude of error is acceptable in decision-making irrigation. Therefore, 40 and 20 random sampling sites should be chosen for predicting the mean soil water content with errors of 5% and 10%, respectively. Additionally, this result can be applied to other center pivot irrigation systems in this region with similar irrigated area, soil property and climate, and this method of determining the random sampling number can also be used for other field scale sites.

CONCLUSIONS

Field experiments were conducted to measure the soil water content at different stages of the irrigation cycle. The changes in soil water content with time during the irrigation cycle were relatively substantial, but the level of spatial heterogeneity of the soil water content was relatively stable. When the soil water content was relatively low, the level

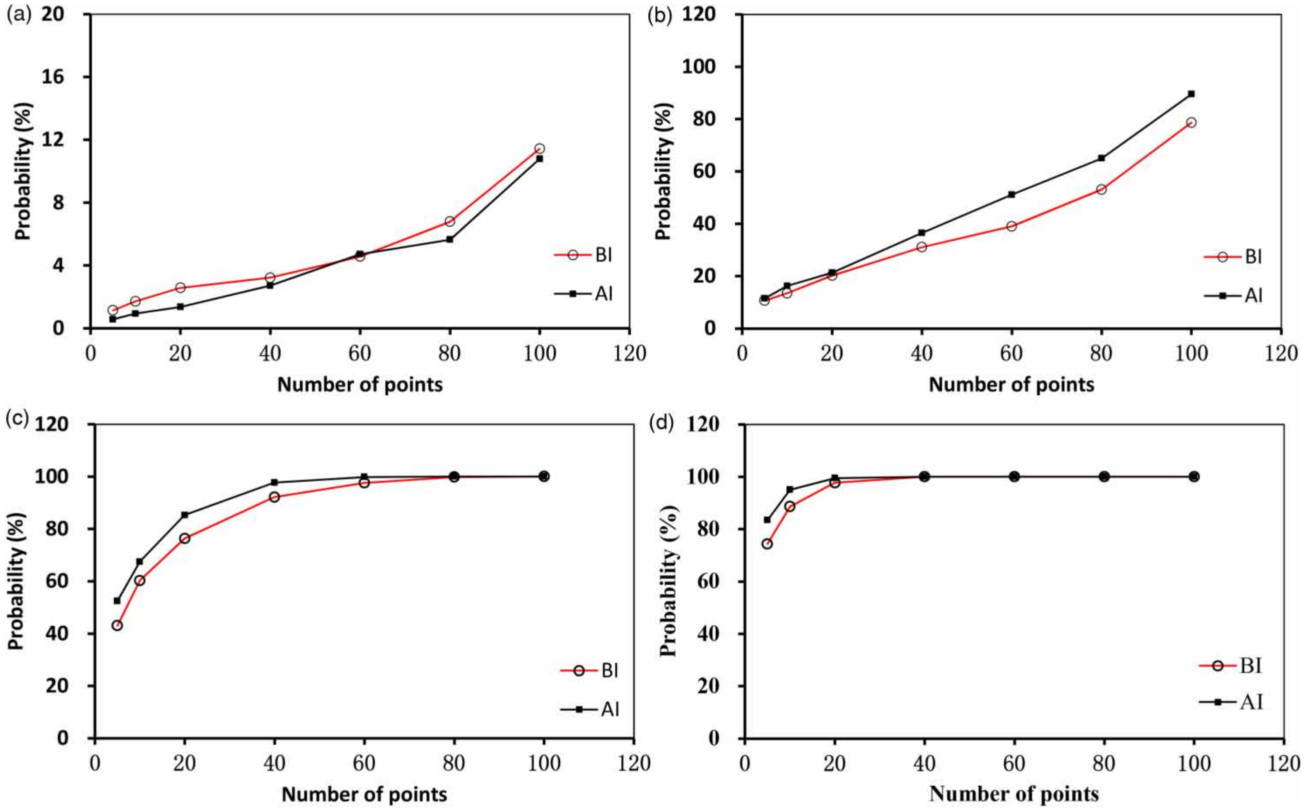

Figure 7 | The probability of the real value of mean soil water content with different random sampling number under the condition of different errors at AI and BI stages. (a) Error 0%; (b) error 1%; (c) error 5%; (d) error 10%.

of spatial heterogeneity of the soil water content tended to be higher. The nugget/sill ratios in a fitted semivariogram model indicated that the soil water content had moderate spatial dependence at the BI stage but weak spatial dependence at the AI stage. At a soil depth of 0–20 cm, the autocorrelation distance of the soil water content was about 70 m at the AI stage and about 140 m at the BI stage, but at a soil depth of 20–40 cm the autocorrelation distance was about 60 m at both the AI stage and the BI stage. The predicted mean soil water content had a relatively smaller error at the BI stage than that at the AI stage when the same number of sampling points was selected.

ACKNOWLEDGEMENTS

This research was supported financially by the National Natural Science Foundation of China (Grant No. 51609197), CAS 'Light of West China' Program (Grant No. XAB2016AW06), Programme of Introducing Talents of Discipline to Universities (No. 104-451115012), and Scientific Research Program of Education Department in Shaan Xi Province (No. 16JS084).

REFERENCES

Bertuzzi, P., Bruckler, L., Bay, D. & Chanzy, A. 1994 Sampling strategies for soil water content to estimate evapotranspiration. *Irrigation Science* **14** (3), 105–115.

Brocca, L., Melone, F., Moramarco, T. & Morbidelli, R. 2010 Spatial-temporal variability of soil moisture and its estimation across scales. *Water Resources Research* **46** (2), W02516.

Burgess, T. M. & Webster, R. 1980 Optimal interpolation and isarithmic mapping of soil properties: I. The Semivariogram and Punctual Kriging. *Journal of Soil Science* **31** (2), 315–331.

Cambardella, C. A., Moorman, T. B., Parkin, T. B., Karlen, D. L., Novak, J. M., Turco, R. F. & Konopka, A. E. 1994 Field-scale variability of soil properties in central Iowa soils. *Soil Science Society of America Journal* **58** (5), 1501–1511.

Choi, M. & Jacobs, J. M. 2011 Spatial soil moisture scaling structure during soil moisture experiment 2005. *Hydrology Processes* **25** (6), 926–932.
Delhomme, J. P. 1978 Kriging in the hydrosciences. *Advances in Water Resources* **1**, 251–266.
Famiglietti, J. S., Ryu, D., Berg, A. A., Rodell, M. & Jackson, T. J. 2008 Field observations of soil moisture variability across scales. *Water Resources Research* **44** (1), W01423.
FAOSTAT 2018 Food and Agriculture Organization of the United Nations. Statistics division. http://www.fao.org/faostat/en/#data/QC; accessed 25 December 2018.
Fu, W., Tunney, H. & Zhang, C. 2010 Spatial variation of soil nutrients in a dairy farm and its implications for site-specific fertilizer application. *Soil and Tillage Research* **106** (2), 185–193.
Hupet, F. & Vanclooster, M. 2002 Intraseasonal dynamics of soil moisture variability within a small agricultural maize cropped field. *Journal of Hydrology* **261** (1–4), 86–101.
Kerry, R. & Oliver, M. A. 2007 Comparing sampling needs for variograms of soil properties computed by the method of moments and residual maximum likelihood. *Geoderma* **140** (4), 383–396.
Li, T., Hao, X. & Kang, S. 2014 Spatiotemporal variability of soil moisture as affected by soil properties during irrigation cycles. *Soil Science Society of America Journal* **78** (2), 598–608.
Long, J., Liu, Y., Xing, S., Qiu, L., Huang, Q., Zhou, B. & Zhang, L. 2018 Effects of sampling density on interpolation accuracy for farmland soil organic matter concentration in a large region of complex topography. *Ecological Indicators* **93**, 562–571.
Longchamps, L., Khosla, R., Reich, R. & Gui, D. W. 2015 Spatial and temporal variability of soil water content in leveled fields. *Soil Science Society of America Journal* **79** (5), 1446–1454.
López-Vicente, M., Quijano, L. & Navas, A. 2015 Spatial patterns and stability of topsoil water content in a rainfed fallow cereal field and Calcisol-type soil. *Agricultural Water Management* **161**, 41–52.
Meyles, E., Williams, A., Ternan, L. & Dowd, J. 2003 Runoff generation in relation to soil moisture patterns in a small Dartmoor catchment, southwest England. *Hydrology Processes* **17** (2), 251–264.
Miller, B. A., Koszinski, S., Hierold, W., Rogasik, H., Schröder, B., Oost, K. V., Wehrhan, M. & Sommer, M. 2016 Towards mapping soil carbon landscapes: issues of sampling scale and transferability. *Soil and Tillage Research* **156**, 194–208.
Robertson, G. P. 2008 *GS+: Geostatistics for the Environmental Sciences*. Gamma Design Software, Plainwell, MI, USA.
Satchithanantham, S., Krahn, V., Ranjan, R. S. & Sager, S. 2014 Shallow groundwater uptake and irrigation water redistribution within the potato root zone. *Agricultural Water Management* **132**, 101–110.
Souza, Z. M. D., Souza, G. S. D., Júnior, J. & Pereira, G. T. 2014 Number of samples in geostatistical analysis and kriging maps of soil properties. *Ciência Rural* **44** (2), 261–268.
Starr, G. C. 2005 Assessing temporal stability and spatial variability of soil water patterns with implications for precision water management. *Agricultural Water Management* **72** (3), 223–243.
Usowicz, B. & Lipiec, J. 2017 Spatial variability of soil properties and cereal yield in a cultivated field on sandy soil. *Soil and Tillage Research* **174**, 241–250.
Utset, A. M., Ruiz, E., Herrera, J. & Ponce de Leon, D. 1998 A geostatistical method for soil salinity sample site spacing. *Geoderma* **86** (1), 143–151.
Wang, J., Fu, B., Qiu, Y., Chen, L. & Wang, Z. 2001 Geostatistical analysis of soil moisture variability on Da Nangou catchment of the loess plateau, China. *Environmental Geology* **41** (1–2), 113–120.
Wang, C., Zuo, Q. & Zhang, R. 2008 Estimating the necessary sampling size of surface soil moisture at different scales using a random combination method. *Journal of Hydrology* **352** (3–4), 309–321.
Wang, J., Yang, R. & Bai, Z. 2015 Spatial variability and sampling optimization of soil organic carbon and total nitrogen for Minesoils of the Loess Plateau using geostatistics. *Ecological Engineering* **82**, 159–164.
Warrick, A. W. & Nielsen, D. R. 1980 Spatial variability of soil physical properties in the field. In: *Applications of Soil Physics* (D. Hillel, ed.), Academic Press, New York, pp. 319–344.
Western, A. W., Zhou, S. L., Grayson, R. B., McMahon, T. A., Blöschl, G. & Wilson, D. J. 2004 Spatial correlation of soil moisture in small catchments and its relationship to dominant spatial hydrological processes. *Journal of Hydrology* **286** (1–4), 113–134.

First received 5 June 2019; accepted in revised form 3 January 2020. Available online 21 January 2020